

The influence of differently substituted cyclopentadienyl Cp^R ligands on the reactivity of [Cp^RFe(CO)₂]₂ with yellow arsenic

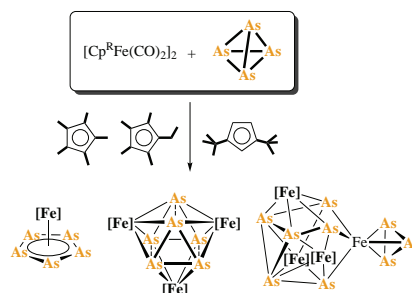
Hannes Krauss, Gábor Balázs, Michael Seidl and Manfred Scheer*

Institute of Inorganic Chemistry, University of Regensburg, D-93040 Regensburg, Germany.

E-mail: manfred.scheer@chemie.uni-regensburg.de

DOI: 10.1016/j.mencom.2022.01.013

The influence of differently substituted cyclopentadienyl Cp^R ligands on the reaction outcome of [Cp^RFe(CO)₂]₂ (Cp^R = C₅Me₅, EtC₅Me₄, 1,3-Bu₂C₅H₃) with As₄ is examined. For C₅Me₅ and EtC₅Me₄, the pentaarsaferrocene derivatives [Cp^RFe(η⁵-As₅)] are formed together with [(Cp^RFe)₃As₆] and [(Cp^RFe)₃As₆{(η³-As₃)Fe}], while for 1,3-Bu₂C₅H₃ only [(Cp^RFe)₃As₆] is formed. The reaction of [(Me₅C₅Fe)₃As₆{(η³-As₃)Fe}] with Tl⁺ leads to [(Me₅C₅Fe)₃As₆Fe]₂(μ,η³:η³-As₃)²⁺ representing an unexpected dicationic cluster.



Keywords: yellow arsenic, iron complexes, cyclopentadienyl ligands, polyarsenic ligand complexes, oxidation.

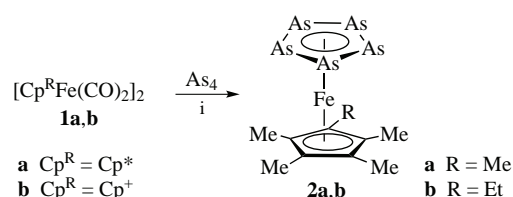
Activation of small molecules in order to achieve a more ecological and atom-efficient way to synthesize compounds of industrial interest is one of the main topics of current research.¹ Beside the activation of N₂ or H₂, the activation of white phosphorus (P₄) is of special interest for the synthesis of organophosphorus derivatives.^{2–5} In order to circumvent the classical conversion of P₄ to PCl₃ followed by treatment with Grignard or organolithium reagents, the direct functionalization of P₄ is desirable.^{6,7} Transition metal complexes containing labile ligands easily activate P₄ under photolytic or thermolytic reaction conditions, leading to complexes containing polyphosphorus ligands (P_n ligands). One of such prominent P_n ligands is the pentaphosphaferrocene [Cp*Fe(η⁵-P₅)], which was synthesized by the reaction of [Cp^RFe(CO)₂]₂ (Cp^R = Cp* = C₅Me₅) **1a** with P₄ at elevated temperatures. Compound [Cp*Fe(η⁵-P₅)] shows a manifold reactivity ranging from coordination,⁸ redox,⁹ electrophilic¹⁰ and nucleophilic¹¹ functionalization. While the synthesis and reactivity of [Cp*Fe(η⁵-P₅)] are well investigated, the corresponding arsenic derivative, pentaarsaferrocene [Cp*Fe(η⁵-As₅)], has far less been studied. This is mainly due to the difficulties in the generation and handling of yellow arsenic As₄ as the starting material, which is highly light-sensitive and practically cannot be stored as a substance. An exception is As₄ if loaded on a carbon-based porous material, which is light-stable.¹² This possibility was, however, discovered only recently. In some cases, a different reactivity compared to its phosphorus congener becomes apparent.¹³ In 1989, the pentaarsaferrocene derivatives [Cp^RFe(η⁵-As₅)] [Cp^R = Cp* = C₅Me₅ (**2a**), Cp⁺ = C₅Me₄Et (**2b**)] were synthesized by Scherer *et al.* via the reaction of As₄ with [Cp^RFe(CO)₂]₂ in boiling decalin in 11 and 12% yields, respectively.¹⁴ Since the yields of these derivatives were rather low, the comprehensive investigation of their reactivity is strongly hampered. Therefore, we were interested in exploring the effect of different reaction conditions and the influence of different cyclopentadienyl ligands on the outcome of the reaction

between [Cp^RFe(CO)₂]₂ and As₄. Herein we report the influence of the Cp^R ligand nature on the formation of the pentaarsaferrocene derivatives [Cp^RFe(η⁵-As₅)] [Cp^R = Cp* = C₅Me₅ (**2a**), Cp^R = Cp⁺ = EtC₅Me₄ (**2b**), Cp^R = Cp'' = 1,3-Bu₂C₅H₃ (**2c**)] as well as the isolation and characterization of the previously unknown by-products that are accessible in these reactions such as [(Cp^RFe)₃As₆] [Cp^R = Cp* (**3a**), Cp⁺ (**3b**), Cp'' (**3c**)] and [(Cp^RFe)₃As₆{(η³-As₃)Fe}] [Cp^R = Cp* (**4a**), Cp⁺ (**4b**)].

For the synthesis of pentaarsaferrocenes, yellow arsenic As₄ is needed. Therefore, an apparatus for its preparation in solution has to be set up.¹⁵ Gray arsenic was evaporated at temperatures above ~630 °C, and the resulting vapor of As₄ was blown by a stream of inert argon into a solvent of choice (in this particular case, decalin). Afterwards the dimeric compounds [Cp^RFe(CO)₂]₂ [Cp^R = Cp* (**1a**), Cp⁺ (**1b**)] were co-thermolized with yellow arsenic in decalin as a high-boiling solvent (Scheme 1).

The reported yields for the preparation of compounds **2a,b** of 11 and 12%, respectively, could be reproduced.¹⁴ Unfortunately, all attempts to improve them by optimizing the reaction time or temperature were unsuccessful. If the reaction temperature is higher and/or the reaction time longer than 90 min, decomposition to the respective ferrocene derivatives [Cp^RFe] takes place. At lower temperatures or shorter reaction times, the conversion of **1a,b** is not complete.

As the known pentaarsaferrocenes were prepared, several questions arose, whether the low conversion of **1a,b** to **2a,b** of ~10% indicates the formation of further products that have not



Scheme 1 Reagents and conditions: i, decalin, 190 °C, 90 min.

yet been identified, and whether it would be possible to use bulkier Cp^R ligands with other substituents to vary the properties of the resulting pentaarsaferrocenes **2**. The reaction of [Cp^RFe(CO)₂]₂ **1c** (Cp^R = C₅H₃Bu₂) with As₄ was expected to introduce the sterically more demanding Cp^R ligand in these derivatives and provide answers to these questions. When applying the same reaction conditions (decalin, 90 min) for the reaction of **1c** with As₄, the expected [Cp^RFe(η⁵-As₅)] **2c** was not obtained after column chromatographic work-up. Instead, the unknown neutral cluster compound [(Cp^RFe)₃As₆] **3c** was isolated in 17% yield (Scheme 2). Compound **3c** contains a central As₆ prism the square faces of which are each capped by a {Cp^RFe} fragment.

Since instead of pentaarsaferrocene a new compound was formed in the thermolysis reaction of **1c** with yellow arsenic, we further attempted the isolation of side products which are possibly formed during the synthesis of **2a,b**. When the reaction mixture is worked up by column chromatography with hexane, the pentaarsaferrocenes **2a,b** are isolated as green fractions. However, further elution with toluene gave brown fractions from which single crystals were obtained. X-ray diffraction (XRD) studies showed the formation of [(Cp^RFe)₃As₆{(η³-As₃)Fe}] [Cp^R = Cp* (**4a**), Cp⁺ (**4b**)] (see Scheme 2). Compound **4a** reported by Hänisch *et al.*¹⁶ was synthesized *via* the reaction of As₇(SiMe₃)₃, FeCl₂, and LiCp*. Additionally, in the latter reaction, along with **4a**, ionic compound [(Cp^RFe)₃As₆]⁺[FeCl₃(thf)]⁻ was obtained; its cation may be regarded as the product of formal oxidation of the Cp^R derivative [(Cp^RFe)₃As₆] **3c**. ¹H NMR investigations of the supernatant mother liquors, from which crystals of compounds **4a** and **4b** were obtained, showed that, in addition to the sharp signals of products **4a,b**, other broad signals were present. Based on the ¹H NMR characteristics of **3c**, these can be assigned to analogous compounds [(Cp^RFe)₃As₆] [Cp^R = Cp* (**3a**), Cp⁺ (**3b**)]. All attempts to isolate **3a,b** from their mixtures with **4a,b** failed due to their very similar solubilities. If the mixtures are repeatedly subjected to column chromatography, compounds **3a,b** decompose. However, the employment of essentially long column provided isolation of analytically pure samples of **4a,b**.

In summary, the reaction of **1a–c** with As₄ leads to several products, *i.e.* the Cp* and Cp⁺ derivatives **1a,b** react to give **2a,b** and **4a,b**, while the Cp^R-substituted derivative **1c** gives exclusively **3c**. The yields given in Scheme 2 were determined by the resulting weights and ¹H NMR spectra of the isolated solids (for the ratio between **3** and **4**) after the column chromatographic work-up of the reaction solution and are related to the used starting material **1a–c**.

The novel compound **3c** was obtained by reacting **1c** with As₄ in boiling decalin (see Scheme 2), followed by column

chromatographic work-up with toluene as eluent. From the concentrated solution at –30 °C, brown crystals of **3c** can be isolated in 17% yield. Compound **3c** is poorly soluble in hexane and CH₂Cl₂, but moderately soluble in toluene. Its intensively colored brown solutions are very air-sensitive, but can be stored for a longer time under an inert atmosphere. In the ¹H NMR spectrum, only two broad signals at δ 1.13 and 10.19 ppm could be detected due to its paramagnetic nature. This explains the signal broadening in the ¹H NMR spectrum and the strong downfield shift of the signal at δ 10.19 ppm. Due to the integral ratios and the position of the signals, the signal at 1.13 ppm is assigned to the *tert*-butyl groups of the Cp^R ligands and the signal at 10.19 ppm to the hydrogen atoms on the Cp ring. The signal intensities do not match the expected values exactly, which can be attributed to the different relaxation times of protons in paramagnetic compounds. In the EI mass spectrum of **3c**, the molecular ion peak was detected in addition to peaks corresponding to fragments such as [(Cp^RFe)₃As₅]⁺ and [(Cp^RFe)₃As₄]⁺. The results of the elemental analysis deviate from the calculated values by ~3.5% in the carbon content, probably due to the trace impurities of gray arsenic present in the samples. Even with repeated attempts, better results could not be achieved. Compound **3c** crystallizes in the monoclinic space group P2₁/c with two independent molecules in the asymmetric unit [Figure 1(a)].[†] It contains a cluster-like core composed of six arsenic atoms and three iron atoms. The geometry of the central As₆ prism is symmetric with As–As distances of 2.5416(5) to 2.5969(6) Å within the triangular faces. Longer, but also

[†] Crystal data for **3c**. C₃₉H₆₃As₆Fe₃, *M* = 1148.96, monoclinic, P2₁/c, *a* = 12.41380(10), *b* = 24.0436(2) and *c* = 29.2262(3) Å, β = 90.3100(10)°, α = γ = 90°, *V* = 8723.09(13) Å³, *T* = 123(1) K, *Z* = 8, *Z'* = 2, *D*_{calc} = 1.750 g cm⁻³, *F*(000) = 4584, μ(CuKα) = 13.141 mm⁻¹, 39679 reflections measured, 15129 unique (*R*_{int} = 0.0337) which were used in all calculations. The final *wR*₂ was 0.0844 (all data) and *R*₁ was 0.0348 [*I* ≥ 2σ(*I*)].

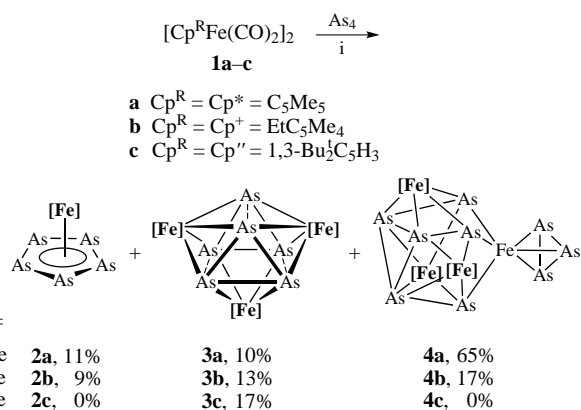
Crystal data for **4a**. C₃₀H₄₅As₉Fe₄, *M* = 1303.34, monoclinic, P2₁/c, *a* = 17.5235(2), *b* = 14.0195(2) and *c* = 15.4107(2) Å, β = 95.8610(10)°, α = γ = 90°, *V* = 3766.17(8) Å³, *T* = 123(1) K, *Z* = 4, *Z'* = 1, *D*_{calc} = 2.299 g cm⁻³, *F*(000) = 2504, μ(CuKα) = 21.065 mm⁻¹, 15529 reflections measured, 5847 unique (*R*_{int} = 0.0467) which were used in all calculations. The final *wR*₂ was 0.0750 (all data) and *R*₁ was 0.0311 [*I* ≥ 2σ(*I*)].

Crystal data for **4b**. C₃₃H₅₁As₉Fe₄, *M* = 1345.41, triclinic, P $\bar{1}$, *a* = 9.8819(3), *b* = 11.8419(4) and *c* = 17.4558(6) Å, α = 93.909(3)°, β = 94.778(3)°, γ = 96.367(3)°, *V* = 2016.84(12) Å³, *T* = 123(1) K, *Z* = 2, *Z'* = 1, *D*_{calc} = 2.215 g cm⁻³, *F*(000) = 1300, μ(CuKα) = 19.695 mm⁻¹, 17613 reflections measured, 6450 unique (*R*_{int} = 0.0406) which were used in all calculations. The final *wR*₂ was 0.1035 (all data) and *R*₁ was 0.0381 [*I* ≥ 2σ(*I*)].

Crystal data for **5**. C₁₀₁H₁₀₂Al₂As₁₅Cl₄F₇₂Fe₈O₈, *M* = 4578.18, triclinic, P $\bar{1}$, *a* = 15.8190(5), *b* = 16.4245(6) and *c* = 16.4417(6) Å, α = 60.077(4)°, β = 75.683(3)°, γ = 77.099(3)°, *V* = 3561.9(3) Å³, *T* = 100(1) K, *Z* = 1, *Z'* = 0.5, *D*_{calc} = 2.134 g cm⁻³, *F*(000) = 2217, μ(CuKα) = 12.358 mm⁻¹, 23890 reflections measured, 12217 unique (*R*_{int} = 0.0328) which were used in all calculations. The final *wR*₂ was 0.1094 (all data) and *R*₁ was 0.0424 [*I* ≥ 2σ(*I*)].

Data were collected on a Xcalibur Gemini Ultra diffractometer equipped with a Ruby CCD detector. The crystals were kept at *T* = 123(1) K (**3c**, **4a**, **4b**) or 100(1) K (**5**) during data collection. Data collection and reduction were performed with CrysAlisPro.²⁶ Using Olex2,²⁷ the structures were solved with ShelXT,²⁸ Superflip²⁹ or SIR-97³⁰ and a least-square refinement on *F*² was carried out with ShelXL.³¹ All non-hydrogen atoms were refined anisotropically. Hydrogen atoms at the carbon atoms were located in idealized positions and refined isotropically according to the riding model. Figures were created with Olex2.²⁷

CCDC 2104962–2104965 contain the supplementary crystallographic data for this paper. These data can be obtained free of charge from The Cambridge Crystallographic Data Centre *via* <http://www.ccdc.cam.ac.uk>.



Scheme 2 Influence of the Cp ligand on the reaction of [Cp^RFe(CO)₂]₂ (Cp^R = Cp*, Cp⁺, Cp^R) with As₄. Reagents and conditions: i, decalin, 190 °C, 90 min.

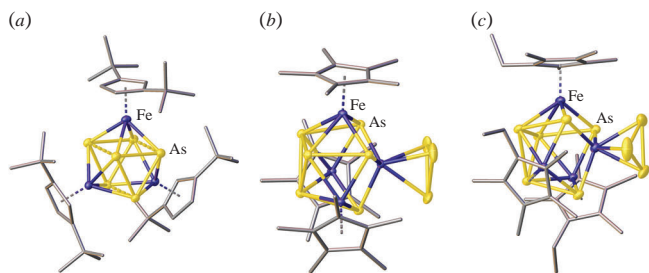


Figure 1 Molecular structures of (a) compound **3c**, (b) compound **4a** and (c) compound **4b** in the solid state. Only one of the two independent molecules of **3c** and only one position of the *cyclo*-As₃ unit of **4b** are depicted. ADPs set to 50% probability level. Hydrogen atoms are omitted for clarity, and carbon atoms are in tube-like representation.

uniform As...As distances are found between the two triangular faces [2.7937(5) to 2.8742(5) Å]. Distances in this range cannot be clearly described as single bonds, but are often found in such cluster compounds.^{16,17} Comparable compounds of the general type [(LM)₃E₆] had already been reported (Table 1).^{18–22}

Clusters of the type [(LM)₃E₆] can be rationalized by the Wade–Mingos concept.^{23,24} The number of valence electrons of the cluster core is also summarized in Table 1. [(Cp*Fe)₃As₆]⁺ is a cationic compound with 20 skeleton electrons and nine skeleton atoms in the cluster, resulting in a *closo*-type core in which the central trigonal prism is formed by four arsenic and two iron atoms. The prism is capped by two additional arsenic atoms and one iron atom. In comparison to compound **3c**, there is one As–As bond missing, but it is compensated by the presence of a short Fe...Fe contact of 2.888 Å (Figure 2).

Apart from the differently substituted Cp^R ligand, compound **3c** has formally the same composition as [(Cp*Fe)₃As₆]⁺, but as a neutral molecule. With an additional electron, however, a completely different structure emerges. The central trigonal prism is formed by six arsenic atoms, while the three iron atoms cap the square surfaces. Furthermore, the cluster should contain 21 skeleton electrons and thus at least one unpaired electron. With regard to the central As₆ prism, compound **3c** is strongly related to [(Cp*Fe)₂(Cp*Co)As₆] or [(Cp^RCo)₃As₆]²⁺, both containing 22 skeleton electrons in the cluster core. However, due to the odd skeleton electron number of **3c**, a classification into *closo* or *nido* type cluster cannot be made. In summary, compound **3c** with 21 skeleton electrons lies exactly in the gap between the already known clusters (see Table 1), but the structure of the Fe₃As₆ core corresponds more to that of the known clusters with 22 skeleton electrons.

Compound [(Cp⁺Fe)₃As₆{(η³-As₃)Fe}] **4b** could be obtained from the reaction of **1b** with As₄ (see Scheme 2). Von Hänisch *et al.* already synthesized the Cp*-substituted analog [(Cp*Fe)₃As₆{(η³-As₃)Fe}] **4a** and characterized it by single-crystal XRD and mass spectrometry.¹⁶ Chromatographic work-up of the reaction solution of **1b** with As₄ affords a brown fraction, which shows in the ¹H NMR spectrum besides the four sharp signals {0.89 ppm (t, CH₂CH₃), 1.76 ppm [s, C₅(CH₃)₂(CH₃)₂(C₂H₅)], 1.79 ppm [s, C₅(CH₃)₂(CH₃)₂(C₂H₅)],

Table 1 Overview of reported compounds of the type [(LM)₃E₆].

Compound	Skeleton electrons	Reference
[(Cp*Fe) ₃ E ₆] ⁺ (E = P, As)	20	16, 18
[(Cp ⁺ Fe) ₃ As ₆] 3c	21	this work
[(Cp ^R Co) ₃ As ₆] ²⁺	22	19
[(Cp*Fe) ₂ (Cp*Co)As ₆]	22	20
[(Cp*Co) ₂ (Mo(CO) ₃)As ₆]	22	21
[(Cp*Co) ₃ E ₆] (E = P, As)	24	20, 22

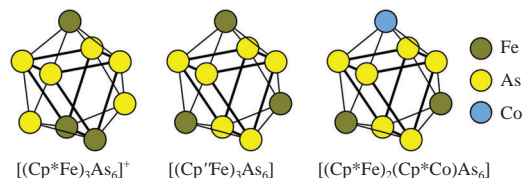


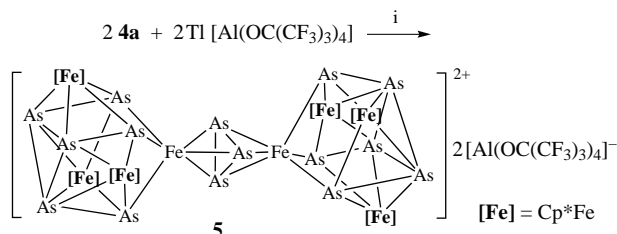
Figure 2 Schematic representation of the central cluster cores in **3c** and the related complexes [(Cp*Fe)₃As₆]⁺ and [(Cp*Fe)₂(Cp*Co)As₆].

2.41 ppm [q, CH₂CH₃]} corresponding to **4b**, four broad signals {1.14 ppm (br, CH₂CH₃), 2.63 ppm (br, CH₂CH₃), 3.15 ppm [br, C₅(CH₃)₂(CH₃)₂(C₂H₅)], 4.16 ppm [s, C₅(CH₃)₂(CH₃)₂(C₂H₅)]} corresponding to the paramagnetic compound **3b**. As expected, the signals for the methyl groups directly attached to the Cp⁺ ligand undergo the largest paramagnetic shift, the three hydrogen atoms of the terminal CH₃ unit of the ethyl group are less influenced.

Based on the integral intensity of the signals in the ¹H NMR spectrum, products **4b** and **3b** are present in a 1:1 ratio. Numerous attempts to separate them failed. Both compounds are poorly soluble in hexane and CH₂Cl₂ and moderately soluble in toluene. The higher lability of **3b** can be employed to isolate **4b** from the mixture by chromatography on a long column when component **3b** would slowly decompose on the column. Experiments showed that ~90 mg of **4b** can be isolated from ~300 mg of a 1:1 mixture in that way. However, with regard to the resulting overall yield of 9% for **4b**, this method can only be considered as an alternative synthetic pathway. ¹H NMR investigations show that **4b** obtained in such a way is sufficiently pure for further reactions. However, since the results of the elemental analysis do not agree with the calculated values, one must bargain for traces of **3b** or gray arsenic to be still present in the solid. In the EI mass spectrum of **4b**, the molecular ion peak as well as further peaks corresponding to the cleavage of the Cp⁺Fe fragment could be detected. Remarkably, there is also a peak corresponding to the fragment As₃⁺ indicating the lability of the terminal *cyclo*-As₃ ligand in **4b**.

Crystals of **4b** suitable for XRD experiments can be obtained from a solvent mixture of toluene/hexane (1:3) at –30 °C. It crystallizes as black platelets in the triclinic space group *P* $\bar{1}$ with two formula units in the unit cell.[†] Under the same conditions, compound **4a** crystallizes in the form of brown rods in the monoclinic space group *P2*₁/*c*.[†] Von Hänisch *et al.* already reported the crystal structure of **4a**, however in their case, **4a** crystallized with one THF molecule per formula unit in the orthorhombic space group *Pnma*.¹⁶ The differences in the Cp^R ligands are only slightly noticeable and the core geometries of **4a, b** are isostructural (see Figure 1). The central structural core represents an Fe₄As₆ polyhedron formally built by the insertion of a {Fe(η³-As₃)} fragment into an As₃-plane of **3**. The As–As distances in this *exo*-As₃ ring are the shortest ones and vary from 2.283(13) to 2.3578(15) Å and are only slightly shorter than the corresponding distances for **4a** [2.3606(9) to 2.3663(9) Å]. All other distances compare well with the corresponding parameters for **4a**. It should be noted that, in contrast to **3c**, all As–As distances are clearly in the range of As–As bonds.

Since product **4a** was obtained in good quantities, we investigated its coordination behavior towards Ti[TEF] [TEF = Al{OC(CF₃)₃}₄]. The coordination of the terminal *cyclo*-As₃ ligand in **4a** to the Ti^I cation was expected. Surprisingly, a redox reaction occurred leading to compound [(Cp*Fe)₃As₆Fe]₂(μ,η³:η³-As₃)[Al(OC(CF₃)₃)₄]₂ **5** (Scheme 3). The reaction was carried out by overlaying a solution of Ti[TEF] in CH₂Cl₂ with a diluted solution of **4a** in toluene. During the reaction, a yellowish white precipitate insoluble in common solvents is formed which could not be



Scheme 3 Reagents and conditions: i, CH_2Cl_2 , toluene, room temperature.

further characterized. The reaction pathway for the formation of **5** is unclear. One possibility would be the oxidation of **4a**, which then dimerizes *via* elimination of arsenic. The resulting precipitate of elemental thallium and gray arsenic should, however, be gray to black, which makes this assumption less probable. Another possibility would be a reaction of TI^+ with **4a** by the cleavage of the *cyclo*- As_3 ligand in the first step. The resulting $\{(\text{Cp}^*\text{Fe})_3\text{As}_6\text{Fe}\}^{2+}$ fragment can then react as a Lewis acid with **4a** leading to **5**.

The amorphous precipitate was removed mechanically from the crystals of **5** by decanting off the mother liquor and washing several times with hexane. Another batch of product could be obtained from the mother liquor by overlaying it with hexane. Compound **5** is poorly soluble in CH_2Cl_2 and THF and insoluble in other common solvents. In its ^1H NMR spectrum, a broad signal at δ 4.36 ppm corresponding to the Cp^* ligand was detected. The strong signal broadening and the downfield shift indicate paramagnetic properties of the dication in **5**. Compared with **4a**, which shows a sharp singlet at δ 1.78 ppm, the resonance signal of **5** is shifted upfield by 2.58 ppm. The $^{19}\text{F}\{^1\text{H}\}$ NMR spectrum reveals a singlet at δ -74.9 ppm for the $[\text{Al}(\text{OC}(\text{CF}_3)_3)_4]^-$ anion. The ESI mass spectrum shows the molecular ion peak of the dication **5** as well as peaks corresponding to the fragments $\{[\text{Cp}^*\text{Fe}]_3\text{As}_6(\text{FeAs}_3)\}^+$ and $\{[\text{Cp}^*\text{Fe}]_3\text{As}_6\}^+$.

Compound **5** crystallizes in the triclinic space group $P\bar{1}$ with two molecules of CH_2Cl_2 and one molecule of toluene in the unit cell (Figure 3).[†] It is formally built up by the combination of two $\{(\text{Cp}^*\text{Fe})_3\text{As}_6\text{Fe}\}$ fragments, derived from **4a**, which are bridged by a *cyclo*- As_3 unit. This forms an inorganic cluster core with a total of eight iron and 15 arsenic atoms. Compound **5** can also be described as a *cyclo*- As_3 triple decker complex of the type $L_n\text{M}(\mu, \eta^3: \eta^3\text{-As}_3)\text{ML}_n$ ($\text{M} = \text{Fe}$). Only one example of this type of complexes was reported, namely $[(\text{triphos})\text{Co}(\mu, \eta^3: \eta^3\text{-As}_3)\text{Co}(\text{triphos})][\text{BPh}_4]_2$ [$\text{triphos} = 1,1,1\text{-tris}(\text{diphenylphosphinomethyl})\text{ethane}$].²⁵

The structure of the starting material **4a** is largely retained in the $\{(\text{Cp}^*\text{Fe})_2\text{As}_6\text{Fe}\}$ subunits of **5**, in which six arsenic atoms form a distorted prism, with each rectangular face being capped by a $\{\text{Cp}^*\text{Fe}\}$ unit. The distances between the arsenic atoms and these capping iron atoms largely agree with those in **4a**, just like the metrical parameters in the *cyclo*- As_3 unit.

In conclusion, we have shown that the nature of the Cp^R ligand plays a decisive role in the reactivity of $[\text{Cp}^R\text{Fe}(\text{CO})_2]_2$ **1**

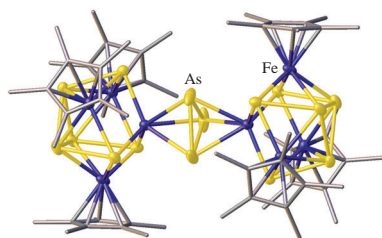


Figure 3 Molecular structure of the dication in **5**. Anions, solvent molecules and hydrogen atoms are omitted for clarity. Carbon atoms are shown in a tube-like representation. ADPs are set to 50% probability level. Only one position of the bridging *cyclo*- As_3 unit is depicted.

with As_4 . While with the Cp^* and Cp^+ ligands the pentaarsaferrocene derivatives $[\text{Cp}^R\text{Fe}(\eta^5\text{-As}_5)]$ **2a, b** and the clusters **3** and **4** are formed, using the sterically more encumbered Cp'' ligand leads to the exclusive formation of $[(\text{Cp}''\text{Fe})_3\text{As}_6]$ **3c**. The first identification of the side-products **3** and **4** and their relative ratio depending on the different substitution pattern of the Cp^R ligand enables a profounder understanding of this system. Furthermore, we could show that complexes such as **4a** can be used for the synthesis of unexpected and more complex clusters such as **5**.

This work was supported by the Deutsche Forschungsgemeinschaft within the project Sche 384/40-1.

Online Supplementary Materials

Supplementary data associated with this article can be found in the online version at doi: 10.1016/j.mencom.2022.01.013.

References

- 1 *Activation of Small Molecules: Organometallic and Bioinorganic Perspectives*, ed. W. B. Tolman, Wiley-VCH, 2006.
- 2 M. Scheer, G. Balázs and A. Seitz, *Chem. Rev.*, 2010, **110**, 4236.
- 3 B. M. Cossairt, N. A. Piro and C. C. Cummins, *Chem. Rev.*, 2010, **110**, 4164.
- 4 M. Caporali, L. Gonsalvi, A. Rossin and M. Peruzzini, *Chem. Rev.*, 2010, **110**, 4178.
- 5 L. Giusti, V. R. Landaeta, M. Vanni, J. A. Kelly, R. Wolf and M. Caporali, *Coord. Chem. Rev.*, 2021, **441**, 213927.
- 6 M. B. Geeson and C. C. Cummins, *Science*, 2018, **359**, 1383.
- 7 M. B. Geeson and C. C. Cummins, *ACS Cent. Sci.*, 2020, **6**, 848.
- 8 E. Peresyppkina, A. Virovets and M. Scheer, *Coord. Chem. Rev.*, 2021, **446**, 213995.
- 9 M. V. Butovskiy, G. Balázs, M. Bodensteiner, E. V. Peresyppkina, A. V. Virovets, J. Sutter and M. Scheer, *Angew. Chem., Int. Ed.*, 2013, **52**, 2972.
- 10 C. Riesinger, G. Balázs, M. Bodensteiner and M. Scheer, *Angew. Chem., Int. Ed.*, 2020, **59**, 23879.
- 11 E. Mädl, M. V. Butovskii, G. Balázs, E. V. Peresyppkina, A. V. Virovets, M. Seidl and M. Scheer, *Angew. Chem., Int. Ed.*, 2014, **53**, 7643.
- 12 A. E. Seitz, F. Hippauf, W. Kremer, S. Kaskel and M. Scheer, *Nat. Commun.*, 2018, **9**, 361.
- 13 M. Schmidt, D. Konieczny, E. V. Peresyppkina, A. V. Virovets, G. Balázs, M. Bodensteiner, F. Riedlberger, H. Krauss and M. Scheer, *Angew. Chem., Int. Ed.*, 2017, **56**, 7307.
- 14 O. J. Scherer, C. Blath and G. Wolmershäuser, *J. Organomet. Chem.*, 1990, **387**, C21.
- 15 M. Seidl, G. Balázs and M. Scheer, *Chem. Rev.*, 2019, **119**, 8406.
- 16 C. von Hänisch and D. Fenske, *Z. Anorg. Allg. Chem.*, 1998, **624**, 367.
- 17 O. J. Scherer, *Acc. Chem. Res.*, 1999, **32**, 751.
- 18 R. Ahlrichs, D. Fenske, K. Fromm, H. Krautscheid, U. Krautscheid and O. Treutler, *Chem. – Eur. J.*, 1996, **2**, 238.
- 19 C. von Hänisch, D. Fenske, F. Weigend and R. Ahlrichs, *Chem. – Eur. J.*, 1997, **3**, 1494.
- 20 G. Friedrich, O. J. Scherer and G. Wolmershäuser, *Z. Anorg. Allg. Chem.*, 1996, **622**, 1478.
- 21 M. Detzel, K. Pfeiffer, O. J. Scherer and G. Wolmershäuser, *Angew. Chem.*, 1993, **105**, 936.
- 22 O. J. Scherer, K. Pfeiffer, G. Heckmann and G. Wolmershäuser, *J. Organomet. Chem.*, 1992, **425**, 141.
- 23 D. M. P. Mingos, *Acc. Chem. Res.*, 1984, **17**, 311.
- 24 K. Wade, *Adv. Inorg. Chem.*, 1979, **18**, 1.
- 25 M. Di Vaira, S. Midollini, L. Sacconi and F. Zanobini, *Angew. Chem., Int. Ed.*, 1978, **17**, 676.
- 26 *CrysAlisPro Software System*, Rigaku Oxford Diffraction, 2020.
- 27 O. V. Dolomanov, L. J. Bourhis, R. J. Gildea, J. A. K. Howard and H. Puschmann, *J. Appl. Crystallogr.*, 2009, **42**, 339.
- 28 G. M. Sheldrick, *Acta Crystallogr.*, 2015, **A71**, 3.
- 29 L. Palatinus and G. Chapuis, *J. Appl. Crystallogr.*, 2007, **40**, 786.
- 30 A. Altomare, M. C. Burla, M. Camalli, G. L. Cascarano, C. Giacovazzo, A. Guagliardi, A. G. G. Moliterni, G. Polidori and R. Spagna, *J. Appl. Crystallogr.*, 1999, **32**, 115.
- 31 G. M. Sheldrick, *Acta Crystallogr.*, 2015, **C71**, 3.

Received: 6th September 2021; Com. 21/6679